Synthesis and Characterization of Layered Zinc Biphenylylenebis(phosphonate) and Three Mixed-Component Arylenebis(phosphonate)/Phosphates

Baolong Zhang, Damodara M. Poojary,† and Abraham Clearfield*

Department of Chemistry, Texas A&M University, College Station, Texas 77843-3255

Received September 30, 1997

Layered zinc 4,4′-biphenylylenebis(phosphonate), $Zn_2(O_3PC_{12}H_8PO_3)\cdot 2H_2O$ (**I**), has been synthesized and its structure solved and refined by using X-ray powder diffraction data. The compound crystallizes in the space group *Pnn*2 with $a = 27.904(1)$ Å, $b = 4.8273(3)$ Å, $c = 5.6450(2)$ Å, and $Z = 2$. The zinc atoms in this compound have distorted octahedral geometry. The phosphonate oxygens bind to zinc through chelation and bridging similar to those found in zinc phenylphosphonate and zinc phenylenebis(phosphonate) reported earlier. The water oxygen atom occupies the sixth coordination site. This paper also reports three mixed zinc arylenebis(phosphonate)/phosphate compounds, $Zn_2(O_3PC_6H_4PO_3)_{0.75}(HPO_4)_{0.5}\cdot 2.5H_2O$ (**II**), $Zn_2(O_3PC_{12}H_8PO_3)_{0.75}(HPO_4)_{0.5}\cdot 2.5H_2O$ (**III**), and $Zn(HO_3PC_{12}H_8PO_3H)_{0.82}(HPO_4)_{0.18}$ (**IV**). Their structures were characterized by X-ray diffraction, IR spectroscopy, solid state ^{31}P NMR spectroscopy, and TGA. It was found that the structures of compounds **II** and **III** are similar to those of their corresponding parent phosphonates but compound **IV** contains a different type of metal−phosphonate framework. BET measurements show that the surface areas of these phosphonates have been largely increased after introducing phosphate groups, mainly however due to mesoporosity.

Introduction

Research on metal phosphonates is undergoing rapid expansion because of their potential application in the areas of sorption and ion exchange, catalysis, and sensors.[1−5] Special interest centers on the layered phosphonates and is due to their unique properties, such as their high thermal stability and the variability of organic functional groups that can be introduced.[6] Originally, work in this area was focused on group IV metal phosphonates.[7] In most cases, these compounds are layered and the metal atoms are bridged by oxygens of the phosphonates, while the organic moiety of the phosphonate projects into the interlayer space.[8,9] By using the reaction of bis(phosphonic acids) with zirconium, the phosphonic acid can bond with metal ions on both ends and thus cross-link inorganic layers to form a molecular sieve-like three-dimensional structure.[10] The distance between the biphenyl cross-links is only 5.3 Å, allowing for no porosity. It was claimed that by the preparation of mixed derivatives in which phosphite or phosphate ions replace some of the biphenyl groups, porosity was built into the structures.[10a,b] The materials prepared by the Dines group were amorphous, and as such, they were able to obtain a complete solid solution series of the type $Zr(O_3PH)_{2-2x}(O_3PC_{12}H_8PO_3)_x$ with $x = 0-1$. Although no pore size measurements were made, they estimated that a micropore of approximate size 8.3×5 Å^2 was present in the particles of average size 0.06 μm.

Because the products were amorphous, little structural information was available. We have attempted to prepare crystalline materials by adding hydrofluoric acid to the reaction mixture. This addition increases the solubility of the phosphonates by formation of the hexafluorozirconium anion, allowing for an Ostwald ripening mechanism to improve the crystallinity. However, in so doing, we were not able to obtain a complete solid solution series because the ratio of phosphate to phosphonate was limited as found earlier for mixed derivatives by Alberti et al.[11] One of the questions that remained unanswered is why the compound containing no phosphite groups exhibited a surface area in excess of 300 m^2 g^{-1}. We recently found that the pore structure of the totally cross-linked products depends on the solvent system.[12] In a DMSO−HF solution, a mixture of micropores and mesopores was obtained and the average pore diameter was about 13 Å. When the DMSO was diluted with benzene, the product contained only mesopores with diameter greater than 50 Å. However, with alcohol−water mixtures, the product obtained had pore sizes of 24−30 Å. Although a hypothesis was advanced to explain this behavior,[12] it is evident

* To whom correspondence should be addressed.
† Present address: Symyx Technologies, 3100 Central Expressway, Santa Clara, CA.

(1) Clearfield, A. In *New Developments in Ion Exchange Materials*; Abe, M., Kataoka, T., Suzuki, T., Eds.; Kodansha, Ltd.: Tokyo, 1991.
(2) Wang, J. D.; Clearfield, A.; Peng, G.-Z. *Mater. Chem. Phys*. **1993**, *35*, 208.
(3) (a) Wan, B.-Z.; Anthony, R. G.; Peng, G.-Z.; Clearfield, A. *J. Catal*. **1986**, *101*, 19. (b) Byrd, H.; Clearfield, A.; Poojary, D. M.; Reis, K. P.; Thompson, M. E. *Chem. Mater*. **1996**, *8*, 2239.
(4) Deniaud, D.; Schollorn, B.; Mansuy, D.; Rouxel, J.; Battioni, P.; Bujoli, B. *Chem. Mater*. **1995**, *7*, 995.
(5) Alberti, G.; Casciola, M.; Palombari, R. *Solid State Ionics* **1993**, *61*, 241.
(6) Clearfield, A. In *Progress in Inorganic Chemistry*; Karlin, K. D., Ed.: John Wiley & Sons, Inc.: NewYork, 1998; Vol. 47.
(7) Alberti, G. In *Comprehensive Supramolecular Chemistry*; Lehn, J. M., Ed.; Pergamon Elsevier Science, Ltd.: Oxford, U.K., 1996; Vol. 7.
(8) Poojary, M. D.; Hu, D. L.; Campbell, F. L., III; Clearfield, A. *Acta Crystallogr*. **1993**, *B49*, 996.
(9) Poojary, D. M.; Zhang, B.; Clearfield, A. *Angew. Chem., Int. Ed. Engl.* **1994**, *33*, 2324.
(10) (a) Dines, M. B.; Di Giacomo, P. D.; Callahan, K. P.; Griffith, P. C.; Lane, R. H.; Cookey, R. E. *ACS Symp. Ser*. **1982**, *192*, 223. (b) Dines, M. B.; Cooksey, R. E.; Griffith, P. C.; Lane, R. H. *Inorg. Chem.* **1983**, *22*, 1003.
(11) Alberti, G.; Costantino, U.; Kornyei, J.; Luciani-Giavagnotti, M. L. *React. Polym.* **1985**, *4*, 1.
(12) Clearfield, A.; Wang, J. D.; Tian, Y.; Campbell, F. L., III; Peng, G.-Z. In *Materials Synthesis and Characterization*; Perry, D., Ed.; Plenum: New York, 1997; p 103.

S0020-1669(97)01238-X CCC: $15.00
Published on Web 04/03/1998

that the acquisition of better defined structural data would help immensely. Therefore, several years ago, we began a systematic study of the zinc and other transition metal phosphonates primarily because of their solubility, which makes it easier to crystallize them[13−15] and in some cases to solve their structures from powder data.[16]

In the interim, Alberti et al.[17] were able to prepare two zirconium pillared phosphonates that were microporous. The strategy employed in preparing an α-layered microporous compound was to use 3,3′,5,5′-tetramethylbiphenyldiphosphonic acid as the pillaring agent together with phosphorous acid as a second ligand. In the α-$Zr(HPO_4)_2$ layer, the phosphate groups are at the corners of essentially equisided parallelograms of length 5.3 Å.[18] The cross section of the methylphosphonic acid is greater than this value, forcing the alternate sites to be occupied by the small phosphite groups. The resultant compound had a surface area of 375 m^2/g with a narrow pore size distribution of between 5 and 6 Å. Alberti et al.[19] were also able to obtain microporous phosphonate pillared zirconium compounds having the γ-layered structure by topotactic ester interchange reactions with γ-zirconium phosphate. Although they were able to obtain unit cell dimensions for both the α and γ derivatives, the crystallinities of the compounds were insufficient to yield the crystal structures. However computer models of the structures were generated.

Recently, we were able to solve the structure of zinc and copper phenylenebis(phosphonate) and biphenylylenebis(phosphonate).[20,21] Zinc and copper phenylenebis(phosphonate) compounds are layered, similar to the corresponding phenylphosphonates, but the inorganic layers are cross-linked by phenylene groups. In the case of biphenylylenebis(phosphonate), however, a linear-chain structure formed. These aryl, fully pillared metal phosphonates are close packed, leaving little space between aryl pillars so that no micropores would be expected. A study on introducing the small phosphate and phosphite groups into the layer structures is being pursued. In this paper, we report the synthesis and characterization of mixed-component zinc phenylenebis(phosphonate)/phosphate and biphenylylenebis(phosphonate)/phosphate. We were also able to synthesize and structurally characterize the layered zinc biphenylylenebis(phosphonate). The effort to synthesize its mixed-component derivative is also reported.

Experimental Section

Materials and Methods. The 1,4-phenylene and 4,4′-biphenylylene bis(phosphonic acids) were prepared according to the reported procedure,[22] with certain modifications.[23] All other chemicals used were of reagent grade quality and were used without further purification. X-ray powder diffraction patterns were taken with a Seifert-Scintag PAD V diffractometer (no internal standard) using nickel-filtered Cu Kα radiation. Solid state ^{31}P NMR spectra were recorded on a Bruker MSL-300 spectrometer. IR spectra were obtained with a Bio-Rad FTS-40 spectrometer by the KBr disk method. Thermogravimetric analyses (TGA) were carried out under an oxygen atmosphere at a heating rate of 10 °C/min with a Du Pont thermal analyst 950 unit. Surface area studies were performed on a Quantachrome Autosorb 6 unit. C, H chemical analyses were performed by Oneida Research Services. Titration curves were recorded with a Tyoto Electronics AT-310 titrimeter by adding 0.05 mL of NaOH every 6 min.

Synthesis of $Zn_2(O_3PC_{12}H_8PO_3)\cdot 2H_2O$ (I). A 0.44 g sample of zinc acetate (2 mmol) in 10 mL of deionized distilled water was mixed with 0.27 g of sodium acetate (2 mmol) in 10 mL of deionized distilled water. A 0.33 g amount of 4,4′-biphenylylenebis(phosphonic acid) was added to 10 mL of water, which resulted in a milky slurry. To this slurry was slowly added the zinc solution. The mixture was transferred to a 100 mL Teflon-lined bomb and heated at 150 °C for 5 days. The product was filtered off and rinsed with deionized water, yielding 0.45 g of white solid after drying in a 60 °C oven for 1 day. Anal. Calcd for $Zn_2(O_3PC_{12}H_8PO_3)\cdot 2H_2O$: C, 30.20; H, 2.52. Found: C, 31.05; H, 2.08.

Synthesis of $Zn_2(O_3PC_6H_4PO_3)_{0.75}(HPO_4)_{0.5}\cdot 2.5H_2O$ (II). A 1.1 g sample of 1,4-phenylenebis(phosphonic acid) (5 mmol) was dissolved in 200 mL of deionized distilled water. To this solution was added 1.36 mL of 85% phosphoric acid (20 mmol). After the pH of this solution was raised to 6.3 by addition of 1 M KOH, 30 mL of $ZnCl_2$ (0.75 M) solution was quickly added. A white solid precipitated immediately. The mixture was then refluxed for 60 h. After filtration, rinsing, and drying in a 60 °C oven for 1 day, 2.18 g of solid was obtained. Anal. Calcd for $Zn_2(O_3PC_6H_4PO_3)_{0.75}(HPO_4)_{0.5}\cdot 2.5H_2O$: C, 13.52; H, 2.13. Found: C, 14.33; H, 2.09.

Synthesis of $Zn_2(O_3PC_{12}H_8PO_3)_{0.75}(HPO_4)_{0.5}\cdot 2.5H_2O$ (III). A 0.78 g sample of 4,4′-biphenylylenebis(phosphonic acid) (2.5 mmol) was dissolved in 100 mL of 0.1 M KOH solution. To this solution was added 1.2 mL of 85% phosphoric acid (17 mmol). While the mixture was stirred, 0.68 g (5 mmol) of $ZnCl_2$ in 20 mL of deionized distilled water was slowly added. A white solid precipitated immediately. The slurry was refluxed at 100 °C for 3 days. A 1 g yield of white solid was obtained after filtering, rinsing, and drying at 60 °C for 1 day. Anal. Calcd for $Zn_2(O_3PC_{12}H_8PO_3)_{0.75}(HPO_4)_{0.5}\cdot 2.5H_2O$: C, 23.67; H, 2.52. Found: C, 23.78; H, 2.28.

Synthesis of $Zn(HO_3PC_{12}H_8PO_3H)_{0.82}(HPO_4)_{0.18}$ (IV). A 0.16 g (0.5 mmol) sample of 4,4′-biphenylylenebis(phosphonic acid) was added to a 50 mL of the solution of deionized distilled water and 0.408 mL (6 mmol) of 85% phosphoric acid. To this was added 30 mL of 0.23 M $ZnCl_2$ solution (7 mmol). The reaction was carried out in a Teflon-lined bomb at 160 °C for 3 days. The solid was filtered off, rinsed with deionized distilled water, and dried (yield = 0.2 g). Anal. Calcd for $Zn(HO_3PC_{12}H_8PO_3H)_{0.82}(HPO_4)_{0.18}$: C, 34.88; H, 2.47. Found: C, 34.83; H, 2.00.

Titration of Compound IV and $Zn(HO_3PC_{12}H_8PO_3H)$. A 50 mg quantity of each compound was added to 50 mL of 0.1 N NaCl, and the solution was titrated with 0.1 N NaOH until the pH was greater than 9.5.

X-ray Powder Data Collection for Compound I. Step-scanned X-ray powder data for the sample (side-loaded into a flat aluminum sample holder) were collected on the finely ground sample by means of a Rigaku computer-automated diffractometer. The X-ray source was a rotating anode operating at 50 kV and 180 mA with a copper target and graphite-monochromated radiation. Data were collected between 3 and 80° in 2θ with a step size of 0.01° and a count time of 12 s/step. The $K\alpha_2$ contribution was mathematically stripped from the data, and peak picking was conducted by a modification of the double-derivative method.[24] The powder pattern was indexed by Ito methods[25] on the basis of the first 20 observed lines. The best solution (FOM = 17)

(13) (a) Martin, K. J.; Squattrito, P. J.; Clearfield, A. *Inorg. Chim. Acta* **1989**, *155*, 7. (b) Cao, G.; Lee, H.; Lynch, V. M.; Mallouk, T. E. *Inorg. Chem.* **1988**, *27*, 2781. (c) Cao, G.; Mallouk, T. E. *Inorg. Chem.* **1991**, *30*, 1434.
(14) (a) Zhang, Y.-P.; Clearfield, A. *Inorg. Chem.* **1992**, *31*, 2821. (b) Cao, G.; Lynch, V. M.; Swinnea, S. J.; Mallouk, T. E. *Inorg. Chem.* **1990**, *29*, 2112.
(15) Wang, R.-C.; Zhang, Y.; Hu, H.; Frausto, R. R.; Clearfield, A. *Chem. Mater.* **1992**, *4*, 864.
(16) Poojary, D. M.; Clearfield, A. *J. Am. Chem. Soc.* **1995**, *117*, 11278.
(17) Alberti, G.; Costantino, U.; Marmottini, F.; Vivani, R.; Zappeli, P. *Angew. Chem., Int. Ed. Engl.* **1993**, *32*, 1357.
(18) Clearfield, A.; Smith, G. D. *Inorg. Chem.* **1969**, *8*, 431. Troup, J. M.; Clearfield, A. *Inorg. Chem.* **1977**, *16*, 3311.
(19) Alberti, G.; Costantino, U.; Marmottini, F.; Murcia-Mascaros, S.; Vivani, R. *Angew. Chem., Int. Ed. Engl.* **1994**, *33*, 1594.
(20) Poojary, D. M.; Zhang, B.; Bellinghausen, P.; Clearfield, A. *Inorg. Chem.* **1996**, *35*, 5254.
(21) Poojary, D. M.; Zhang, B.; Bellinghausen, P.; Clearfield, A. *Inorg. Chem.* **1996**, *35*, 4942.
(22) Allinger, N. L. *Organic Chemistry*; Worth: NewYork, 1980.
(23) Bellinghausen, P. M.S. Thesis, Texas A&M University, Dec 1995.
(24) Mellory, C. L.; Synder, R. L. *Adv. X-ray Anal.* **1979**, *23*, 121.
(25) Visser, J. W. *J. Appl. Crystallogr.* **1969**, *2*, 89.

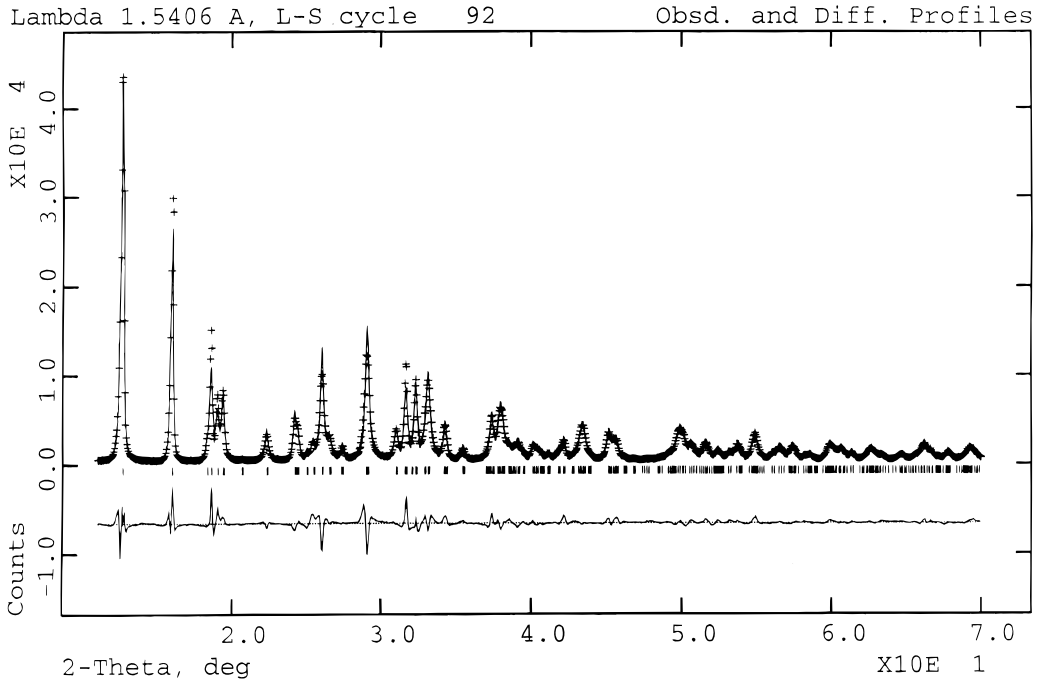

Figure 1. Observed (+) and calculated (−) profiles for the Rietveld refinement of compound **I**. The difference plot is on the same intensity scale.

which indexed all the peaks of compound **I**, indicated an orthorhombic cell with lattice parameters $a = 27.904(1)$, $b = 4.8273(3)$, and $c = 5.6450(2)$ Å. The systematic absences were consistent with the space group *Pnn*2 or its centrosymmetric equivalent. On the basis of the molecular symmetry, the noncentric space group was chosen for structure solution.

Structure Solution and Refinement of Compound I. The in-plane unit cell dimensions in this case are similar to those obtained for Zn($O_3PC_6H_5$)·H_2O.[13a,b] Therefore, a structural model for the layers (Zn−O_3PC) in the present compound was developed on the basis of the structure of Zn($O_3PC_6H_5$)·H_2O, by taking into account the symmetry and molecular geometry. This model was used as a starting set of parameters for the Rietveld refinement and structure completion.

Refinement of the structure was carried out using the program GSAS.[26] Intially, the parameters such as zero-point error, scale factor, lattice parameters, terms for background, and peak shape functions were refined. The positional parameters were then refined with soft constraints. As indicated earlier, the coordination about the Zn atom is a distorted octahedron. Therefore, no constraints were applied to the O−O-nonbonded distances about the Zn polyhedron. However, in the initial stages of refinement, the Zn−O distances were constrained to a value of 2.12(3) Å. The P−O and P−C bond distances were held at 1.53(1) and 1.80(1) Å, respectively. The phosphonate groups were constrained to the tetrahedral geometry by giving appropriate values for O···O and O···C nonbonded contacts. A series of difference Fourier maps computed at this stage revealed the positions of two of the carbon atoms of the biphenylylene group; the other atoms were obtained by a modeling study. Constrained refinement of the phenylene group was carried out by assigning a value of 1.39(1) Å for the C−C bonds. The distance between two carbon atoms bonded to a carbon atom whose angle was to be constrained to 120° was held to a value of 2.39(1) Å. The C−C bond connecting the two phenylene groups was held at a distance of 1.47(1) Å. As the refinement progressed, the weights for the soft constraints were reduced, but they could not be removed without distorting the structure, particularly the geometry of the organic groups. All the atoms were refined isotropically. A correction was made for the preferred orientation effect by using the March−Dollase method[27] in the GSAS suite of programs. The diffraction vector in the present case is along the a^* axis. No corrections were made for absorption effects. A final Rietveld refinement plot is given in Figure 1. In this figure, the first peak was excluded because it is huge and asymmetric, and therefore the profile coefficients used to refine this peak will not fit other peaks well.

Table 1. Crystallographic Data for Compound **I**

formula	$C_{12}H_{12}O_8P_2Zn_2$
fw	476.92
space group	*Pnn*2 (No. 34)
a (Å)	27.904(1)
b (Å)	4.8273(3)
c (Å)	5.6450(2)
V (Å^3)	760.4
Z	2
d_{calc} (g/cm^3)	2.08
μ (cm^{-1})	6.23
pattern range in 2θ (deg)	10−70
no. of unique reflns	191
no. of structure params	54
R_{wp}	0.135
R_p	0.107
R_f	0.024

Results

Structure of $Zn_2(O_3PC_{12}H_8PO_3)\cdot 2H_2O$. Crystallographic data are given in Table 1. Selected bond parameters are listed in Table 2. The layer arrangement is shown in Figure 2, and the projection of the structure down the *b* axis is presented in Figure 3. A 2-fold axis lies at the center of the C−C bond connecting the two phenyl groups. Due to this symmetry, the asymmetric unit contains only six independent carbon atom positions, C1−C6, corresponding to the biphenylene group. The two PO_3 groups of the bis(phosphonate) are also symmetry related. The biphenylene groups cross-link the inorganic layers whose mean planes are located in the *bc* plane at $x \cong 0.25$ and 0.75. The zinc atoms are six-coordinated by five oxygens of the phosphonate groups and one oxygen of the water molecule. All the phosphonate oxygens take part in metal binding, and among them, two oxygens are involved in both chelation and bridging. Oxygens O1 and O3 chelate the metal and at the same time bridge the unit-cell-translated Zn atoms along the *c*-axis

(26) Larson, A.; von Dreele, R. B. *GSAS*: *Generalized Structure Analysis System*; Los Alamos National Laboratory: Los Alamos, NM, 1985.
(27) Dollase, W. A. *J. Appl. Crystallogr*. **1986**, *19*, 267.

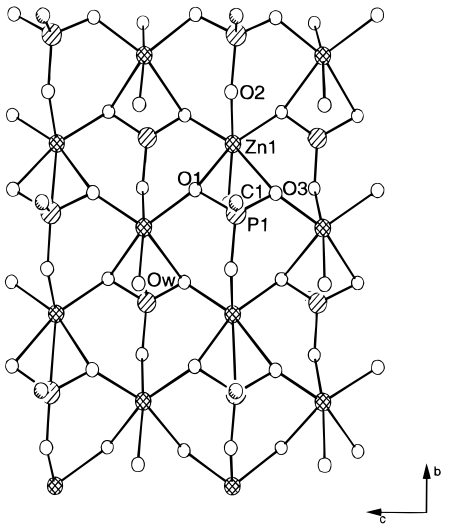

Figure 2. Layer arrangement in the structure of compound **I** showing the in-layer connectivity.

Table 2. Bond Lengths (Å) and Bond Angles (deg) for Compound (I)

Zn−O1	2.320(10)	Zn−O1	2.049(9)
Zn−O2	2.094(8)	Zn−O(W)	2.173(8)
Zn−O3	2.441(10)	Zn−O3	1.974(10)
P1−O1	1.555(10)	P1−O2	1.544(7)
P1−O3	1.493(10)	P1−C1	1.820(7)
C1−C2	1.410(7)	C1−C6	1.419(7)
C2−C3	1.435(7)	C3−C4	1.409(7)
C4−C4	1.398(6)	C4−C5	1.413(7)
C6−C5	1.414(7)		
O1−Zn−O1	159.0(5)	O1−Zn−O2	93.1(5)
O1−Zn−O2	81.4(6)	O1−Zn−O3	63.0(2)
O1−Zn−O3	96.9(6)	O1−Zn−O3	96.5(6)
O1−Zn−O3	103.5(3)	O1−Zn−O(W)	86.7(5)
O2−Zn−O(W)	168.0	O2−Zn−O3	85.2(6)
O2−Zn−O3	91.3(6)	O3−Zn−O3	159.9(7)
O3−Zn−O(W)	90.7(8)	O1−P1−O2	105.2(9)
O1−P1−O3	109.5(6)	O1−P1−C1	109.9(6)
O2−P1−C1	107.5(5)	O2−P1−O3	111.8(8)
O3−P1−C1	112.7(9)	P1−C1−C2	120.7(7)
P1−C1−C6	122.1(7)	C1−C2−C3	114.6(7)
C2−C1−C6	115.7(7)	C3−C4−C4	121.4(7)
C3−C4−C5	112.7(6)	C4−C4−C5	120.6(5)
C4−C5−C6	115.4(7)	C1−C6−C5	114.7(7)

direction. The zinc atoms along the *b* axis are linked by the third oxygen of the phosphonate, O2, to form a metal−phosphate layer in the *bc* plane. The sixth coordination site is completed by the oxygen atom (O4) of the water molecule. The Zn−O2 bond distance (2.094(8) Å) is normal. The Zn−O bond lengths within the chelate ring are longer {Zn−O1 = 2.320(10), Zn−O3 = 2.441(10) Å} than the bond lengths corresponding to the same oxygens involved in the bridging interaction {Zn−O1 = 2.049(9), Zn−O3 = 1.974(10) Å}. The bond distance involving the water oxygen is 2.173(8) Å. The bond angle in the chelation ring, O1−Zn−O3, is 63.0(2)°, and the trans angles are 159.0(5)°. This type of zinc−oxygen−phosphorus connectivity is very similar to that in zinc phenylphosphonate.[13a,b]

The metal−phosphate layers are cross-linked by biphenylylene groups. These rings are separated by 5.6450(2) Å along the *c* axis and 4.8273(3) Å along the *b* axis. The C−C contact distance between two adjacent biphenylene rings is around 3.6−3.8 Å. This arrangement results in severe nonbonded hydrogen interactions. Two phenyl rings in the biphenyl group are thus not in the same plane but are inclined to each other by about 62°.

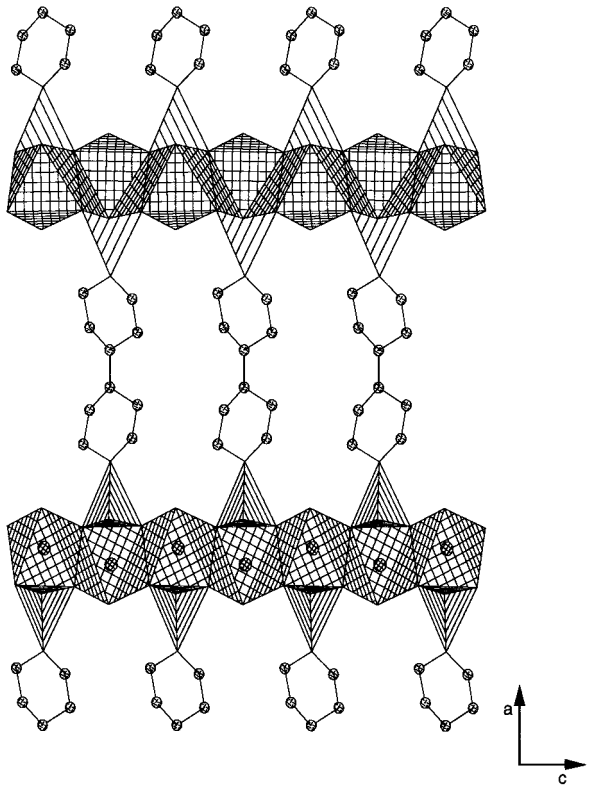

Figure 3. Projection of the structure of compound **I** down the *b* axis showing the bridging nature of the diphosphonate groups.

The structure of compound **I** is similar to that of zinc phenylenebis(phosphonate).[20] In zinc phenylenebis(phosphonate), four of the coordination sites are occupied by the symmetry-related position of the oxygen atom. This oxygen is involved in chelating and bridging zinc atoms. The second oxygen (corresponding to O2) links zinc atoms along the *b* axis to form a layer. All bond lengths and angles are very close to the values observed in compound **I**.

In the structure of zinc phenylenebis(phosphonate), solved earlier[20] in space group *Pnnm*, the phenylene rings are constrained by the 2/*m* symmetry which forces them to align parallel to the *ac* plane. An effort was made to change the symmetry from *Pnnm* to the noncentric space group *Pnn*2, in which the phenylene groups are not constrained by the mirror symmetry and hence the rings are free to rotate about the P−C bond. However, the refinement in this space group did not converge. In the structure solution and refinement of compound **I**, we utilized the data in both the centric and acentric space groups but convergence was achieved only in *Pnn*2.

X-ray Diffraction Study of Compounds II−IV

Figure 4b shows the X-ray powder pattern of compound **II**, and for comparison the X-ray powder pattern of its parent zinc phenylenebis(phosphonate) is shown in Figure 4a. The two patterns are very similar except for some minor changes in the intensities of some reflections indicating that the structural skeleton of zinc phosphonate remains intact while some of the phenylene phosphonates are replaced by phosphate groups as shown schematically in Figure 5. The XRD pattern of compound **III** also shows such a similarity to its parent zinc phosphonate (**I**) (Figure 6a,b). However, all of the peaks are broad, indicating strong phase disorder caused by introducing the phosphate groups. Unlike those of compounds **II** and **III**, the X-ray diffraction pattern of compound **IV** (Figure 7b) is

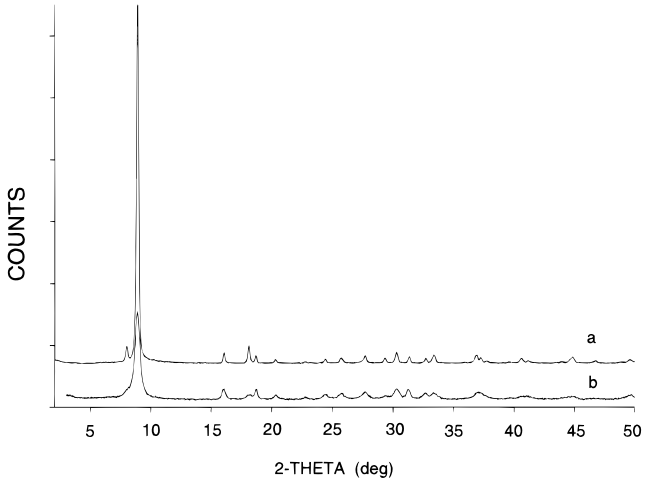

Figure 4. X-ray powder patterns of zinc phenylenebis(phosphonate) (a) and compound **II** (b).

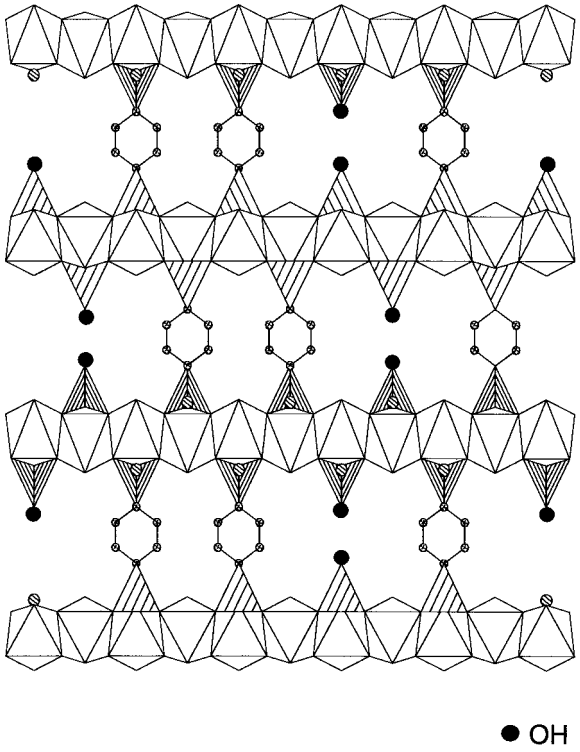

Figure 5. Schematic representation showing the substitution of phosphonate groups by phosphate groups.

quite different from that of its parent linear-chain zinc phosphonate $Zn(HO_3PC_{12}H_8PO_3H)$[20] (Figure 7a), and the first diffraction peak has a *d* spacing of 14.9 Å compared to 14.17 Å for $Zn(HO_3PC_{12}H_8PO_3H)$. This change in *d* spacing and other features of the pattern indicate that the structure of **IV** may not be the same as that of the linear-chain compound.

Spectroscopic Results

Figure 8a shows the ^{31}P NMR spectrum of zinc phenylenebis(phosphonate). It has a single peak at 22.9 ppm, corresponding to the phosphorus of the phosphonate group. Compound **I** shows the corresponding resonance at 24 ppm, which indicates that the phosphorus atoms of the biphenylylenebis(phosphonate) are in an environment similar to that found in monophenyl compound. Since compound **II** was prepared in the presence of phosphoric acid, its ^{31}P NMR spectrum (Figure 8b), besides

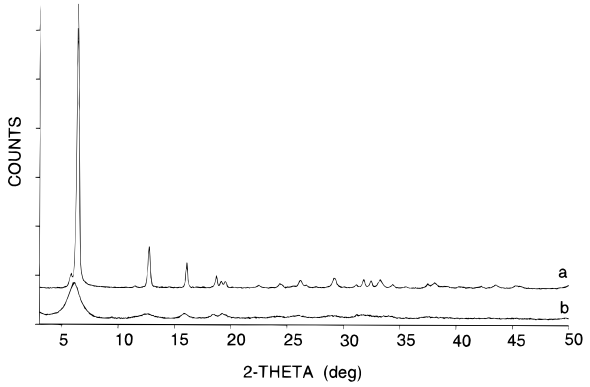

Figure 6. X-ray powder patterns of compounds **I** (a) and **III** (b).

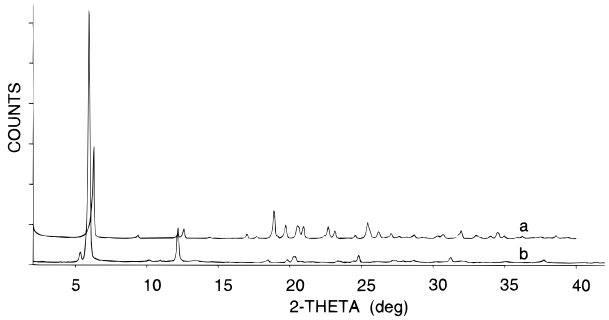

Figure 7. Comparison of X-ray powder patterns of linear-chain zinc biphenylylenebis(phosphonate) with (b) and without (a) the presence of phosphate.

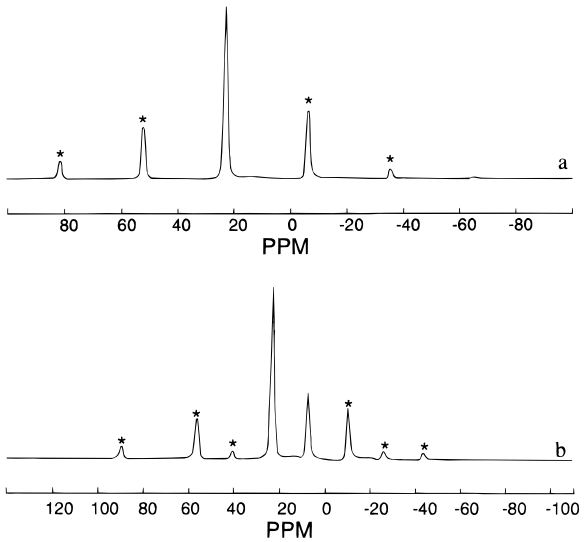

Figure 8. Solid-state MAS ^{31}P NMR for zinc phenylenebis(phosphonate) (a) and compound **II** (b). The spinning sidebands are indicated by asterisks.

a peak at 23.2 ppm, contains a new peak at 7.5 ppm, which is attributed to monohydrogen phosphate. The spectrum of compound **III** is similar to that of compound **II**, suggesting that it also contains both phosphate and phosphonate groups. Compound **IV** was prepared under conditions similar to those employed for the synthesis of the linear-chain compound $Zn(HO_3PC_{12}H_8PO_3H)$,[20] but with the presence of phosphoric acid. In its spectrum, besides the peak at 7.5 ppm due to phosphate, the resonance of phosphonate is at 23.5 ppm. This is considerably different from the ^{31}P peak in the NMR spectrum of $Zn(HO_3PC_{12}H_8PO_3H)$, which occurs at 17 ppm, adding additional evidence that compound **IV** has a different structure.

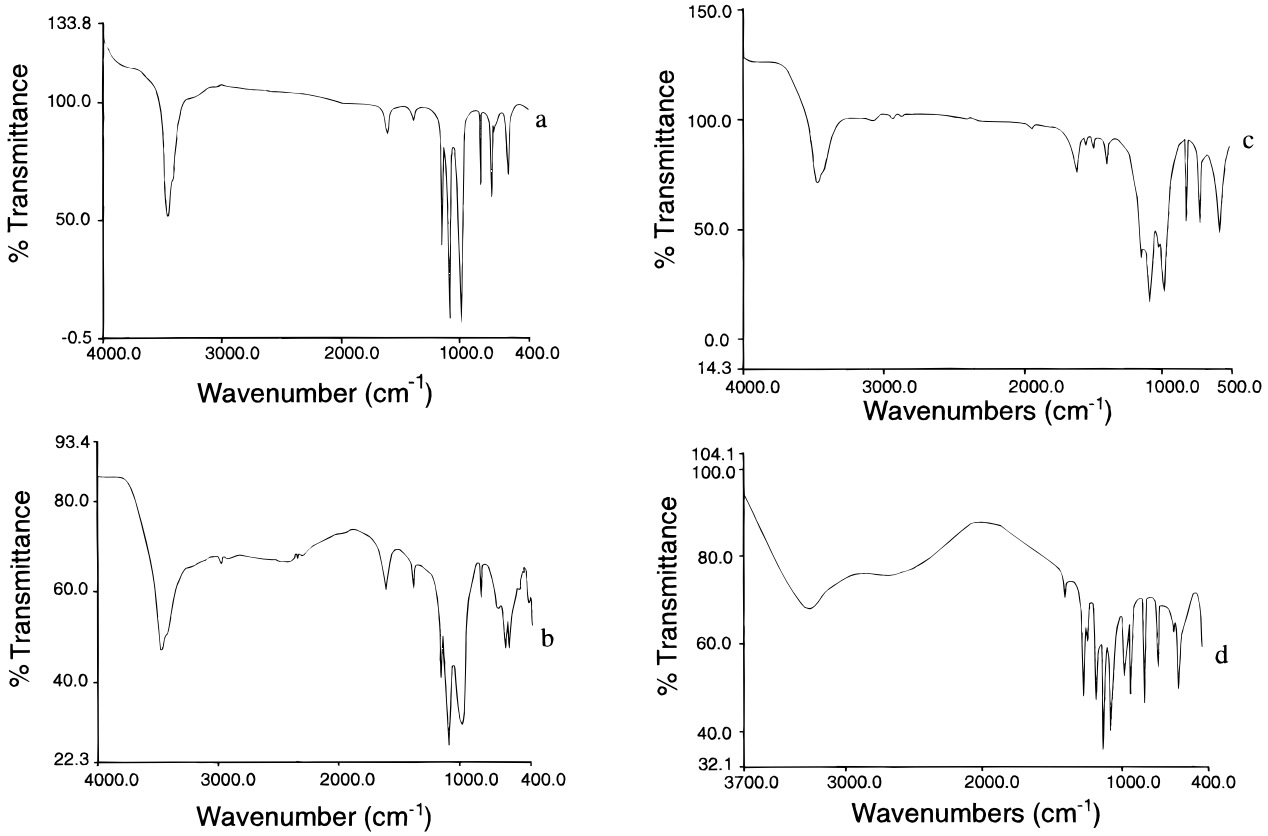

Figure 9. Infrared spectra of compounds **I** (a), **II** (b), **III** (c), and **IV** (d).

One of the characteristic bands in the IR spectrum of the layered zinc phenylenebis(phosphonate) is a doublet at 3460 and 3430 cm^{-1} arising from the O−H stretching vibrations of water coordinated to zinc atoms. These two bands appear in the spectra of compounds **I**−**III** (Figures 9a−c), indicating that these compounds all have cooordination water similar to that of zinc phenylenebis(phosphonate). The other common prominent bands in the spectra of compounds **I**−**III** are three peaks at 1145, 1089, and 986 cm^{-1}, which are attributed to $R-PO_3^{2-}$ phosphonate stretching vibrations. Because of the presence of phosphate in compounds **II** and **III**, the peak at 983 cm^{-1} becomes broad (shoulder at around 980 cm^{-1}) relative to this peak for phenylenebis(phosphonate). Like the phenylenebis(phosphonate), compound **II** has an absorption band at 835 cm^{-1} because of the out-of-plane vibrations of para-substituted phenylene rings, whereas this band for compounds **I** and **III** is at 817 cm^{-1}. The spectrum of compound **IV** (Figure 9d) is more like that of the linear-chain zinc biphenylylenebis(phosphonate).[20] It has a broad band centered at 3222 cm^{-1}, which is due to O−H stretchings of hydrogen-bonded hydroxyl groups. The adsorptions at 1201, 1144, and 1077 cm^{-1} are due to the phosphonate and phosphate stretching vibrations. It is this region of the spectrum that differs from that of the linear-chain compound even though several of the weaker bands coincide.

Thermogravimetric Study

The thermogravimetric weight loss curves for the pure zinc phosphonate phases and their corresponding mixed phosphonate−phosphate derivatives are shown in Figures 10−12 for compounds **III**, **II**, and **IV**, respectively. Compound **I** begins to lose its coordinated water at 108 °C. The observed weight loss for this stage is 6.86%, close to the calculated value 7.55%

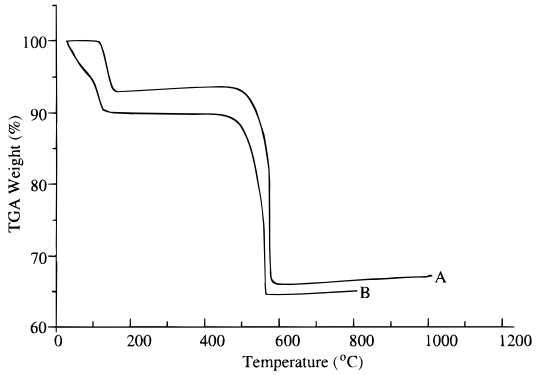

Figure 10. TGA traces of compound **I**, $Zn_2(O_3PC_{12}H_8PO_3)\cdot 2H_2O$ (A), and compound **III**, $Zn_2(O_3PC_{12}H_8PO_3)_{0.75}(HPO_4)_{0.5}\cdot 2.5H_2O$ (B).

for loss of two water molecules. After dehydration, there is no weight loss or phase change (observed from DTA data) until the temperature reaches 473 °C. In the temperature range 473−607 °C the organic moieties decompose. On the assumation that the final product is $Zn_2P_2O_7$, the reactions may be represented as in eq 1. The total weight loss was found to be

$$Zn_2(O_3PC_{12}H_8PO_3)(H_2O)_2 \xrightarrow{108-162\ ^\circ C,\ -2H_2O} Zn_2(O_3PC_{12}H_8PO_3) \xrightarrow[O_2]{473-607\ ^\circ C,\ O_2} Zn_2P_2O_7 + 12CO_2 + 4H_2O \quad (1)$$

33.8% as compared to a calculated value of 36.1%. The corresponding mixed-derivative (compound **III**) behaved similarly (Figure 10B) except that the water loss began as soon as heating was initiated and occurred in two steps. The first, due to interstitial or surface water, is not present in the pure zinc

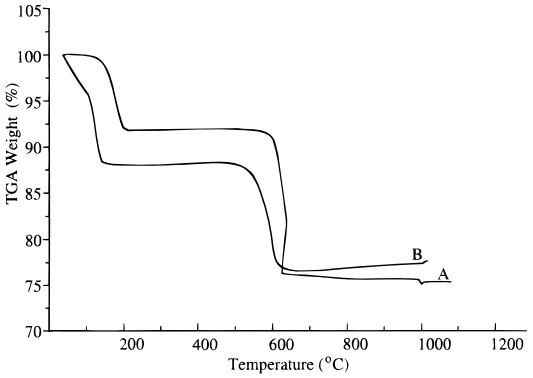

Figure 11. TGA traces of zinc phenylenebis(phosphonate), $Zn_2(O_3PC_6H_4PO_3)(H_2O)_2$ (A), and compound **II**, $Zn_2(O_3PC_6H_4PO_3)_{0.75}(HPO_4)_{0.5}\cdot 2.5H_2O$ (B).

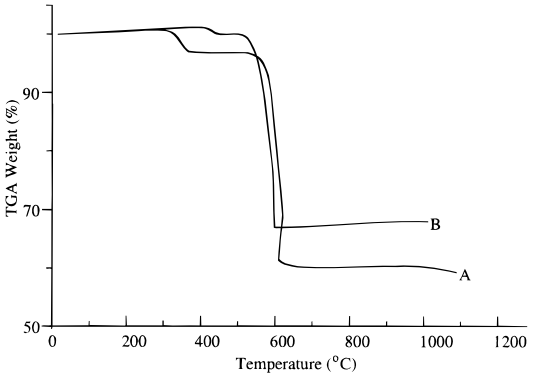

Figure 12. TGA traces of the linear-chain biphenylylenebis(phosphonate), $Zn(H_3OPC_{12}H_8PO_3H)$ (A), and compound **IV**, $Zn(H_3OPC_{12}H_8PO_3H)_{0.82}(HPO_4)_{0.18}$ (B).

bis(phosphonate) because of its hydrophobic nature and the fact that the water molecules are coordinated to the zinc atoms.[20] The second step occurs immediately after most of the interstitial water is lost and, in analogy with compound **I**, is attributed to water coordinated to Zn. The total observed weight loss from the water is 9.75%, a value close to that calculated for 2.5 mol of water (9.86%).

The TGA curve for $Zn_2(O_3PC_6H_4PO_3)(H_2O)_2$, shown in Figure 11A, was taken from ref 20. The coordinated water is lost at 110−200 °C and amounts to 8.6% (calculated 8.98%). The total weight loss is 24.4% compared to a calculated value of 24.0%. The mixed phosphate−phosphonate (compound **II**) shows a two-step weight loss of water that amounts to 11.75% compared to a calculated value of 11.28% based upon a water content of 2.5 mol. The higher water content in both this example and the one above is due to the introduction of the more hydrophilic monohydrogen phosphate group and the more openness of the structure. The decrease in stability of compounds **II** and **III**, as shown by the lower temperature of burnout of the organic is also attributed to the introduction of the phosphate groups, which allows oxygen ready access to the interior. The TGA curve of compound **IV** is similar to that for the linear-chain zinc biphenylenebis(phosphonate), $Zn(HO_3PC_{12}H_8PO_3H)$ (Figure 12B,A). It shows no weight loss up to 389 °C, which is 104 °C higher than the parent linear-chain phosphonate, indicating that compound **IV** is more thermally stable. The first weight loss is due to condensation of the hydroxyl groups and is followed by decomposition of the phenyl rings. The total weight loss for the parent compound amounts to 40.4%, while the calculated weight loss for this process is 40.8%, assuming that the end product is zinc phosphite, $Zn(PO_3)_2$ (eq 2). The total observed weight loss for the mixed phosphonate−phosphate was 34.5% as compared to a calculated value of 37.6%. The formula in brackets in eq 2 is that of an unknown intermediate that is stable to ∼600 °C after the split-out of water from the monohydrogen phosphonate groups.

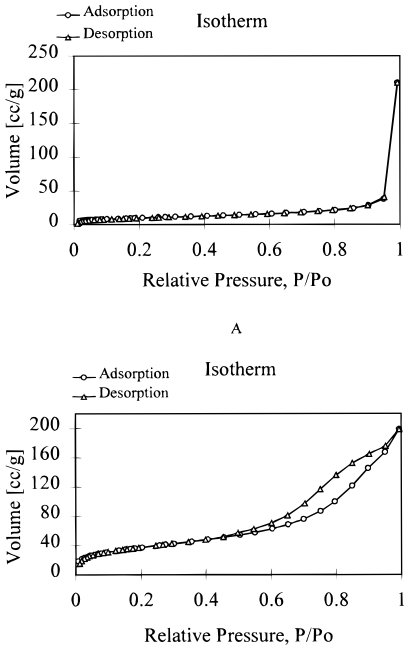

Figure 13. Isotherms of compound **I** (A) and compound **III** (B).

Table 3. BET Surface Area Data for Zinc Phosphonate Derivatives

compound	multi BET SA ($m^2\ g^{-1}$)	Langmuir SA ($m^2\ g^{-1}$)
$Zn_2(O_3PC_6H_4PO_3)\cdot 2H_2O$	28.5	148
II	84	495
I	35	51
III	136	192
$Zn(HO_3PC_{12}H_8PO_3H)$	20	28
IV	51	335

$$Zn(HO_3PC_{12}H_8PO_3H) \xrightarrow{285-355\ ^\circ C,\ -H_2O} [Zn(O_3PC_{12}H_8PO_3)] \xrightarrow{389-609\ ^\circ C,\ O_2} Zn(PO_3)_2 + 12CO_2 + 4H_2O \quad (2)$$

Surface Area and Pore Size

Table 3 lists the surface area of the zinc phosphonates and their mixed-component derivatives. Overall BET and Langmuir surface areas of the mixed-component zinc phosphonate/phosphates are much higher than those of the corresponding pure phosphonates. Parts A and B of Figure 13 show the isotherms of compounds **I** and **III**, respectively. All the isotherms of the pure phosphonates are similar to that shown in Figure 13A, which is typical for nonporous materials. The isotherms of the mixed-component derivatives have a hysteresis loop of the type illustrated by the curve in Figure 13B. This suggests that these compounds have slit-shaped pores and these pores are mostly mesopores. Among these compounds, compound **III** has the largest surface area. The average pore size is about 66 Å in diameter.

Titration Data for Compound IV and $Zn(HO_3PC_{12}H_8PO_3H)$

Compound **IV** was prepared in the same way as the linear-chain compound, $Zn(HO_3PC_{12}H_8PO_3H)$, and thus was thought

to have a similar structure. The zinc atom in this linear-chain compound is tetrahedrally coordinated by oxygens of the phosphonate groups. This lower coordination arises because one of the oxygen atoms of each phosphonate group is not involved in bonding to the zinc ions as it is protonated. The linear chains are actually linked together as double chains that are in turn cross-linked perpendicularly to the chain direction to form layers as shown in Figure 15. The hydrogen bonds between the hydroxyl groups join the layers together to form a loosely held three-dimensional structure. Apparently the use of two rather than three phosphonate oxygens forces a lower metal coordination number and in the process the biphenyl rings rotate to an angle of 52° relative to each other.[20] This diprotonated compound was prepared at a low pH of 1.6. When the pH of the reaction solution is raised to a higher value (4.5), the phosphonate is further deprontonated to form the layered type structure of compound **I**, which is also similar to that of zinc phenylenebis(phosphonate). Compound **I** was also obtained by titrating the linear-chain compound with 0.1 N NaOH to a pH of ~9. The titration curve is shown in Figure 14a. The initial addition of NaOH results in a decrease in pH to 3.4 followed by a plateau of zero slope. This plateau indicates that two solid phases are present and the system has no degrees of freedom. A similar treatment has been reported for the ion exchange reaction exhibited by pure crystalline α-zirconium phosphate,[28] $Zr(HPO_4)_2 \cdot H_2O$. An end point (represented as a circle in the titration curve) was achieved at pH 5.4, which corresponds closely to the neutralization of half the phosphonate protons. The titration curve beyond the end point resembles that expected for a hydrolysis reaction. An X-ray pattern taken of the solid phase obtained at pH 9 revealed it to be zinc biphenylylenebis(phosphonate) dihydrate, $Zn_2(O_3PC_{12}H_8PO_3)(H_2O)_2$. The overall reaction is shown in eq 3.

$$2Zn(HO_3PC_{12}H_8PO_3H) + 4NaOH(aq) \rightarrow Zn_2(O_3PC_{12}H_8PO_3)(H_2O)_2 + Na_4(O_3PC_{12}H_8PO_3) + 2H_2O \quad (3)$$

The same phase transformation does not occur for the linear-chain copper biphenylylenebis(phosphonate)[21] and compound **IV**. One of the reasons may be the stronger hydrogen bonding in these two compounds. The supporting evidence is provided by their titration curves as shown for compound **IV** in Figure 14b. The pH drastically increased at the beginning of the titration until it reached a value of 9.2; then it fell to 8.5 probably due to hydrolytic consumption of base. After this, the pH slowly increased back to 9.2. The major difference between these two titration curves is the pH values at which the plateaus appear. For the zinc linear-chain compound, it occurred at a low pH resulting from the neutralization of the protons of the monohydrogen phosphonate groups. For compound **IV**, however, this deprotonation process is delayed until the pH of the solution reaches a point at which the solid begins to hydrolyze.

Figure 15 shows the phase change from linear-chain to layer type structure through neutralization of the protons of zinc biphenylylenebis(monohydrogenphosphonate). Since the reaction was completed below a pH of 9 and the solid was not visibly seen to dissolve, the reaction must be chemically topotactical. As far as we know, this is the first example of direct solid-state phase transformation in metal phosphonates catalyzed by base. This phase transformation may go through several steps. The first step is neutralization of one of the protons of

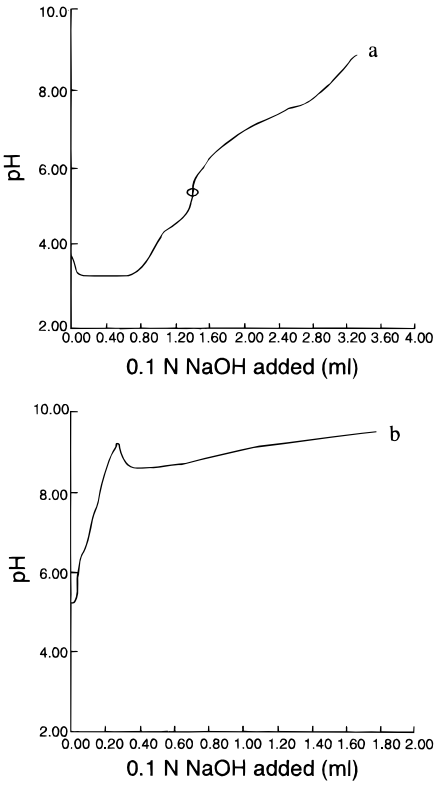

Figure 14. Titration curves of linear-chain zinc biphenylylenebis(phosphonate) (a) and compound **IV** (b).

zinc phosphonate. The end point suggested that 2.8 mequiv/g of protons has been neutralized; the calculated value corresponding to 1 mol of protons/g of sample is 2.6 mequiv/g. This proton may originate from O1 and O2 hydroxyls shown by the dashed line in Figure 15A. The other protonated oxygens are O4 and O5. They are pointing toward the center of the double chains and are involved in hydrogen bonding with each other along the *b* axis. However, the end point for neutralization of this proton is not as clear as the first one. That is because of the hydrolysis of phosphonate at elevated pH. The calculated total value for 2 mol of protons amounts to 5.3 mequiv/g. The titration result shows that 5.6 mequiv/g of protons has reacted at a pH of ~8.

Discussion

The structure of zinc phenylenebis(phosphonate) is layered and similar to the layer structure of zinc phenylphosphonate, $Zn(O_3PC_6H_5)$.[13a,b] They have similar in-layer plane dimensions and layer arrangements. The basal spacings, however, are different. The phenylphosphonate has a bilayer arrangement in which phenyl groups are pointed away from either side of the inorganic layer into the interlayer space; thus the layers actually pack together by van der Waals forces. It is a true two-dimensional layered compound. In the case of zinc phenylenebis(phosphonate), the layers are joined together by phenylenebis(phosphonate) groups to form an ideally three-dimensional network.

However, using similar synthetic methods, we were not able to obtain a layered zinc biphenylylenebis(phosphonate). Instead, the linear-chain compound $Zn(HO_3PC_{12}H_8PO_3H)$ was obtained. This change in structure can now be attributed to the low pH at which the reaction was conducted (1.6), preventing complete ionization of the diphosphonic acid. Apparently the use of two rather than three phosphonate oxygens for bonding forces a

(28) Clearfield, A.; Kullberg, L.; Oskarsson, A. *J. Phys. Chem.* **1974**, *78*, 1150.

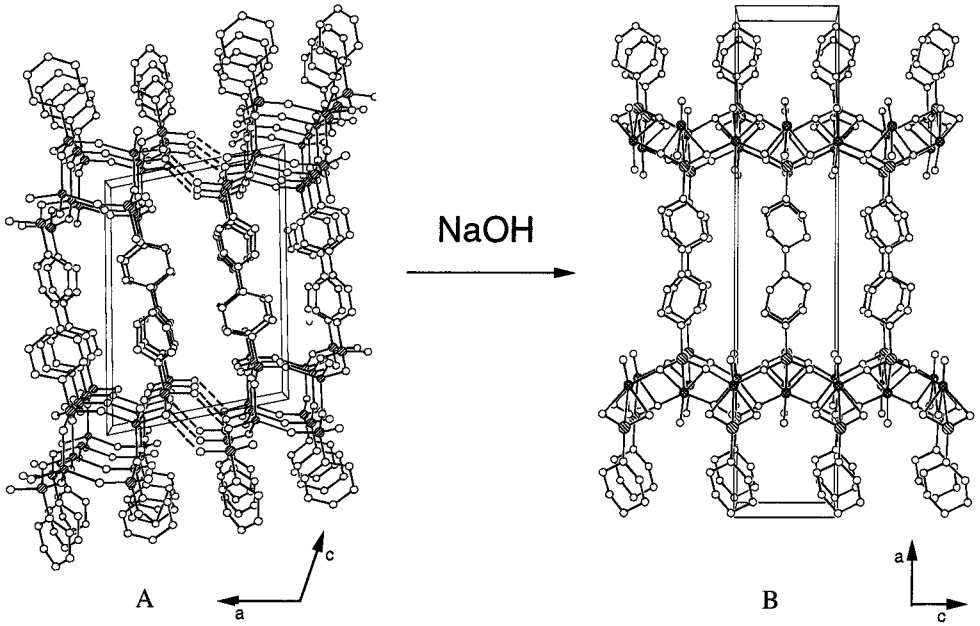

Figure 15. Solid-phase transformation in base from the protonated linear-chain compound $Zn(H_3OPC_{12}H_8PO_3H)$ (A) to layered, cross-linked compound **I**, $Zn_2(O_3PC_{12}H_8PO_3)\cdot 2H_2O$ (B). The hydrogen bonds in the former compound are designated by dashed lines.

lower metal coordination number and in the process the biphenyl rings rotate to an angle of 52° to each other.[20] When the pH of the reaction solution is raised to ~4.5, the phosphonic acid is sufficiently ionized to form the more familiar zinc phenylphosphonate type layer as illustrated in Figures 3 and 15B. However, the biphenyl rings are still rotated relative to each other by ~62°.

Since the phenyl rings are closely packed in the lateral directions in the fully pillared phosphonates, there is little space left between layers, resulting in their very low surface areas. To introduce micropores, our effort was directed toward replacement of some of aryl rings by phosphate groups. However, it is difficult to synthesize single-phase mixed-component compounds because the phosphate and arylphosphonate groups do not like to occupy positions next to each other due to the difference in hydrophobic and hydrophilic characters and the size difference between phosphate and phosphonates. The zinc ion is easier to precipitate with arylenebis(phosphonic acids) than with phosphoric acid. When we used a phosphonate-to-phosphate ratio of 1:1, the compounds obtained were almost pure zinc phosphonates. For phenylenebis(phosphonic acid), when phosphonic acid and phosphoric acid were added in the ratio of 1:4, the end product had a phosphonate-to-phosphate ratio of 3:2. In the case of biphenylylenebis(phosphonate), to obtain the same ratio in the end product as the one in phenylenebis(phosphonate), the starting reactant ratio had to be increased to 7:1. This is probably because the K_{sp} of zinc biphenylylenebis(phosphonate) is much smaller than that of the monophenylenebis(phosphonate) and is therefore easier to precipitate. Further increase of the ratio of phosphoric to phosphonic acid in both cases, while maintaining reasonable crystallinity, often results in formation of zinc phosphate. Additional studies with the phosphite ion and methylphosphonic acid are in progress in an effort to achieve regularity and greater crystallinity in the mixed-ligand compounds.

Compound **III** has the largest surface area among the mixed-component compounds. However, the increase results from formation of mesopores most likely created by disordering the structure. Further attempts to create microporous structures are in progress, and the results will be presented in a subsequent publication.

Acknowledgment. This work was supported by the National Science Foundation under Grant DMR-9107715 and the Robert A. Welch Foundation under Grant A673, for which grateful acknowledgment is made. We thank Dr. Boris Shpeizer for assistance in the collection of surface area data.

Supporting Information Available: Tables of atomic coordinates, isotropic thermal parameters, and an indexed powder pattern for compound **I** (5 pages). Ordering information is given on any current masthead page.

IC9712380